

## QUANTITATIVE CHARACTERIZATION OF IMPACT CRATER MATERIALS ON THE MOON: IMPLICATIONS FOR DEGRADATION PROCESSES AND STRATIGRAPHIC AGE. J. T. Wang<sup>1,2,3</sup>, M. A. Kreslavsky<sup>2</sup>, J. Z. Liu<sup>1,\*</sup>, J. W. Head<sup>4</sup>, and M. M. Kolenkina<sup>5</sup>, <sup>1</sup>Center for Lunar and Planetary Sciences, Institute of Geochemistry, Chinese Academy of Sciences, Guiyang 550081, China (wangjuntao@mail.gyig.ac.cn and liujianzhong@mail.gyig.ac.cn), <sup>2</sup>Earth and Planetary Sciences, University of California – Santa Cruz, Santa Cruz, CA 95064, USA, <sup>3</sup>University of Chinese Academy of Sciences, Beijing 10049, China; <sup>4</sup>Earth, Environmental and Planetary Sciences, Brown University, Providence, RI 02912, USA, <sup>5</sup>MEsLAB, Moscow State University of Geodesy and Cartography (MIIGAiK), Moscow, Russia.

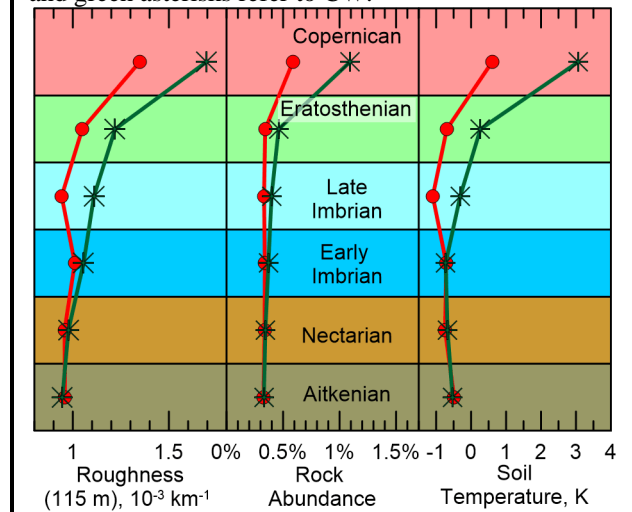
**Introduction:** Impact craters are the most abundant landform on the surface of the Moon. Crater morphology undergoes degradation with age [1]: the sharp morphology of pristine craters becomes subdued due to smaller impacts, mass wasting, lava flooding and proximity weathering from larger craters. Relative (stratigraphic) ages on the Moon are defined according to the lunar geological timescale [2], which is subdivided into Pre-Nectarian Period, which is also dubbed Aitkenian [3], Nectarian Period, Early Imbrian Epoch, Late Imbrian Epoch, Eratosthenian Period, and Copernican Period. The relative ages of lunar geologic units and features, especially craters, have been established by decades of researchers. In early geological maps [4-7], the stratigraphic age was ascribed to craters according to the cross-cutting and superposition relationships, their morphology and state of degradation, and the presence or absence of crater rays. We now have high resolution image and topographic data, and thermal infrared measurements from the Lunar Reconnaissance Orbiter (LRO). From this we can obtain more quantitative attributes of craters and their degradation, such as topographic roughness, night-time soil temperature and rock abundance. Using these quantified measurements, we here report on a preliminary analysis of changes in crater material properties with stratigraphic age, and suggest several cases where the stratigraphic age of a crater might have been misclassified.

**Data:** For the stratigraphic age of the crater, we utilized the 2015 version of the LPI lunar crater database [8] that is reviewed continuously. For each crater assigned a stratigraphic age in the database, we map four crater material subunits [9, 10] based on images and topographic data from LRO mission: central peak material (CP), crater floor material (CF), crater wall material (CW), continuous ejecta (CE, also named crater rim material). We mapped 5000 subunits for 1612 craters and analyzed them.

We used topography data obtained by the Lunar Orbiter Laser Altimeter [11] (LOLA) to calculate roughness at 115 m, 230 m, 460 m, 920 m and 1.8 km baseline. The roughness measure we chose is the “interquartile range of profile curvature” [12]. We also used the thermophysical properties of crater subunits [13] derived from the DIVINER Experiment onboard LRO: rock abundance and night-time soil temperature (with the global latitudinal trend subtracted).

**Degradation of crater material with age:** Fig. 1 summarizes age trends for craters larger than 40 km, thus excluding all simple craters. Craters of younger ages have distinctive roughness and thermophysical properties (Fig. 1), that degrade with age and approach global average values. Despite the conspicuous age trends (Fig. 1) the domains of parameter values for different ages overlap significantly (e.g., Fig. 2), partly due to the natural variability of pristine craters. Therefore roughness and thermophysical parameters alone cannot be used for independent age determination.

**Fig. 1.** Roughness at 115 m baseline, the mean rock abundance, and the median normalized night-time soil temperature as a function of stratigraphic age, which is plotted against the vertical axis in stratigraphic order (the most recent on top). The red circles refer to CE, and green asterisks refer to CW.



**Topographic roughness.** Topographic roughness shows a generalized overview of the textures at smaller scales. The median roughness values calculated over subsets of craters represent a typical roughness for given subunits belonging to a given stratigraphic age. For CF and CW, the roughness value always declines with age at all baselines. We interpret this to occur due to progressive disintegration of materials by smaller impacts and mass wasting. CE shows a significant roughness decrease with age only from the Copernican to Eratosthenian periods. We interpret this to mean that the degradation rate of CE is more rapid early in the history of the crater, and roughness will no longer

change after it reaches a certain level. All the units undergo continuous mass wasting; however CW and CF retain their topography for a long time throughout the degradation process.

For long baselines (not shown in Fig. 1) there is an increasing trend of CE roughness with age, except for the Copernican period; this seemingly contradicts our interpretation of ongoing degradation and reaching equilibrium. We attribute this to an observational bias: for those craters of older age, the CE subunit can be mapped only near the rim of crater; therefore, long-wavelength elevated rim topography affects the roughness signature.

**Rock abundance and soil temperature.** The thermal infrared measurements provide a means of understanding the physical properties of the upper decimeters of the regolith on crater material subunits. Our results (Fig. 1) confirm increased rock abundance and soil temperature for young craters [13,14]. With time, rocks and regolith particles disintegrate due to space weathering factors. For CE, the age trend is observed only for the Copernican (Fig. 1), similarly to the roughness trend.

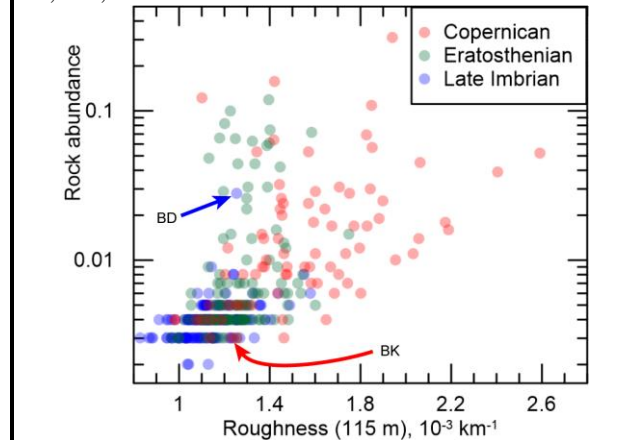
There is an unexpected weak trend of soil temperature increase with increasing age for older crater ages (Fig. 1). Because older craters are systematically larger, we suggest that those larger impact events excavate deeper and initially produce larger blocks; with age, this might result in a slightly greater proportion of rocks and pebbles in the shallow subsurface, even in a thoroughly gardened regolith. This could result in an increase in the night-time temperature.

**Misclassified stratigraphic ages:** The quantitative measurements discussed above can aid in determining the stratigraphic ages of craters. On the other hand, an unusual combination of properties for some craters (e.g., substrate, size, angle of impact, etc.) could explain their seemingly anomalous state. For example, the Late Imbrian crater Bonpland D (BD in Fig. 2) has unusually high soil temperature and rock abundance on its walls, well outside the domain of Late Imbrian craters. In high-resolution images of this crater, we observe that a general rim softness and an apparently thick regolith are indeed consistent with an Imbrian age; however, there are rock boulder tracks and fresh regolith flows [15] on the inner walls, which indicates active processes during the Copernican period.

We also found craters whose stratigraphic age was misclassified in the database. We checked high-resolution images of craters that have been classified as Copernican, but possess too low values of rock abundance, soil temperature, and topographic roughness for such an age (e.g., Bel'kovich K shown in Fig. 2). We found that the morphology of the following craters is inconsistent with a Copernican age: Bel'kovich K, O'Day, Autolycus, Virtanen, Taruntius, Carpenter,

Eudoxus, Mosting, and Birkhoff Z. All of these craters appear older, perhaps Eratosthenian or in some cases, even Imbrian. These craters have morphological signatures of thick regolith: the specific texture of impact melt on the crater floors is not distinguishable, there are few boulders, no signs of geologically recent slides, and the morphology of superimposed meters-size craters suggests a meters-thick loose layer.

**Fig. 2.** Scatter plot of CW rock abundance and roughness at 115 m baseline. Colored dots show individual craters of different stratigraphic ages. BD, Bonpland D; BK, Bel'kovich K.



**Conclusion:** These different types of quantitative data (e.g., topographic roughness, rock abundance and soil temperature) provide additional useful and objective ways to study the subunits of craters of different ages and to assess both misclassified ages and anomalous conditions.

**Acknowledgement:** This work is supported by the Key Research Program of the Chinese Academy of Sciences (Grant NO. XDPB11), the National Key Basic Research Special Foundation of China (Grant No. 2015FY210500), the Key Program of Frontier Science of Chinese Academy of Sciences (Grant No. QYZDY-SSW-DQC028), the Strategic Priority Research Program (B) of the Chinese Academy of Sciences (Grant No. XDB18000000), and the National Natural Science Foundation of China (Grant No. 41773065, 41490634, 41373068).

**References:** [1] Head J. W. (1975) *The Moon*. 12(3), . 299-329. [2] Wilhelms D. E. et al. (1987) *The Geologic History of The Moon*. [3] Guo D. et al. (2016) *LPSC 47*, Abstract #1744. [4] Lucchitta B. K. (1978) *USGS MIS Map I-1062*. [5] Wilhelms D. E. and El-Baz F. (1977) *USGS MIS Map I-948*. [6] Wilhelms D. E. et al. (1979). *USGS MIS Map I-703*. [7] Wilhelms D. E. and McCauley J. F. (1971). *USGS MIS Map I-703*. [8] Losiak A. et al. (2009) *LPSC 40*, Abstract #1532 [9] Liu J. Z. et al. (2016) *LPSC 47*, Abstract #2039. [10] Liu J. Z., et al. (2017) *LPSC 48*, Abstract #1477. [11] Smith D. E. et al. (2010). 150(1), 209-241. [12] Kreslavsky M. A. et al. (2013). *Icarus*. 226(1), 52-66. [13] Bandfield J. L. et al. (2011). *JGR-Planets*. 116(E12). [14] Ghent R. et al. 2016. *Icarus*. 273, 182-195. [15] Kokelaar B. et al. 2017. 122(9), 1893-1925.